**The American Journal of Human Genetics, Volume *98***

## Supplemental Information

# Mutations in Subunits of the Activating Signal Cointegrator 1 Complex Are Associated with Prenatal Spinal Muscular Atrophy and Congenital Bone Fractures

**Ellen Knierim, Hiromi Hirata, Nicole I. Wolf, Susanne Morales-Gonzalez, Gudrun Schottmann, Yu Tanaka, Sabine Rudnik-Schöneborn, Mickael Orgeur, Klaus Zerres, Stefanie Vogt, Anne van Riesen, Esther Gill, Franziska Seifert, Angelika Zwirner, Janbernd Kirschner, Hans Hilmar Goebel, Christoph Hübner, Sigmar Stricker, David Meierhofer, Werner Stenzel, and Markus Schuelke**

## Table of contents

## Supplemental figures

## Supplemental tables

## Morphometric analysis of the sural nerve

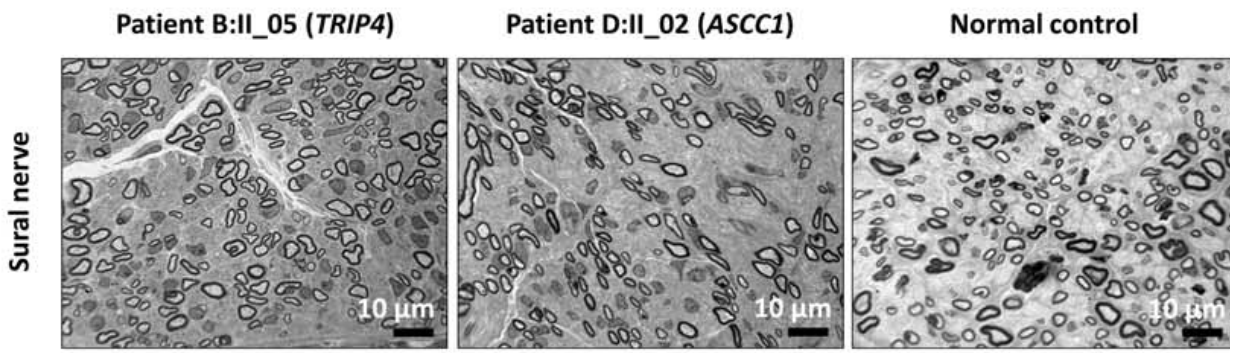


***Figure S1.*** **Representative cross sections of sural nerve biopsy specimens** Five of such visual fields were analyzed for each nerve in two patients and one age-matched control.

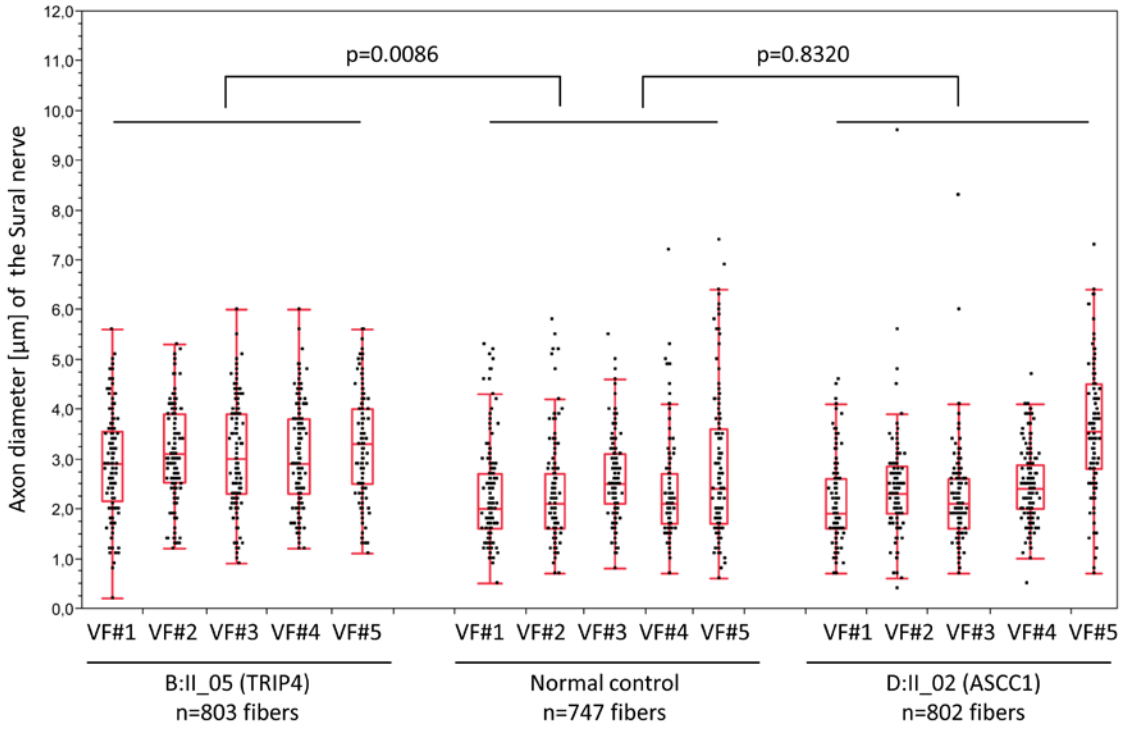


***Figure S2.*** **Morphometric analysis of myelinated axon diameters of sural nerve biopsies.** Sural nerve biopsies were fixed in glutaraldehyde, embedded in Epon®. Semithin sections were stained with methylene blue or with paraphenylene diamine to visualize the myelin sheaths. From each nerve five full visual fields that were entirely filled with myelinated axons were photographed, together with an object micrometer scale using a 100x objective on a Leica DML3000 inverted microscope. The images were recorded in bright field with a cooled SPOT RT3 CCD-camera (1,600 x 1,200 px). Axon diameters were measured morphometrically using the free ImageJ v1.37a program. The axon diameters were depicted in a multiple dot/box blot. The boxes depict the median, $10^{th}$, $25^{th}$, $75^{th}$, and $90^{th}$ percentiles; p-values were calculated with the non-parametric Man-Whitney U-test.

## Results of the autozygosity mapping in three families

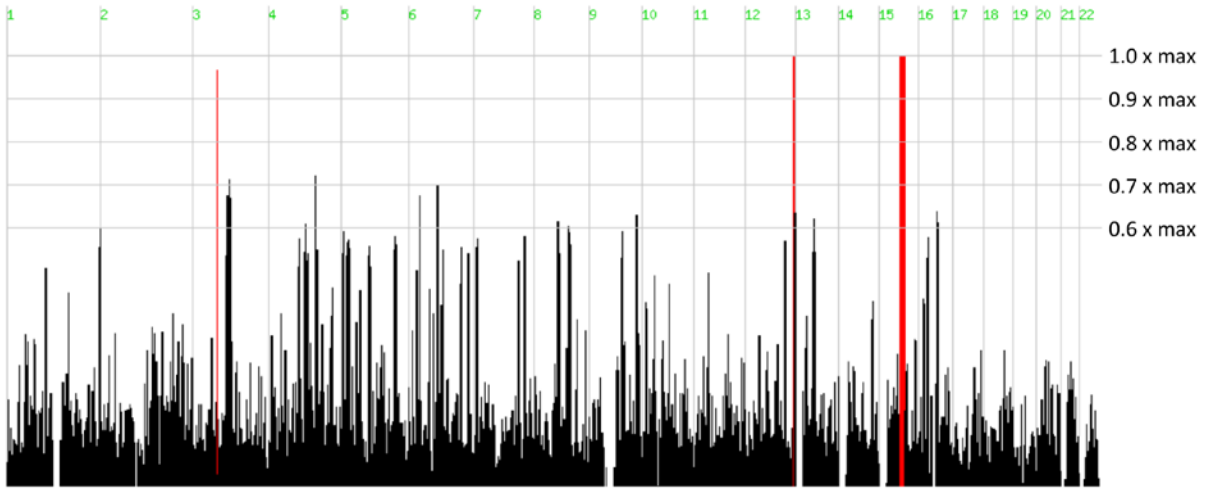


***Figure S3.*** **Autozygosity mapping of Family A** Two affected individuals were used for the analysis. The red bars depict the autozygous regions at: Chr03:64,230,433-65,658,852 (rs3911778-rs6803573), Chr12:129,242,824-132,057,829 (rs7966499-rs7963314), and Chr15:53,697,249-66,260,894 (rs1021746-rs333556).

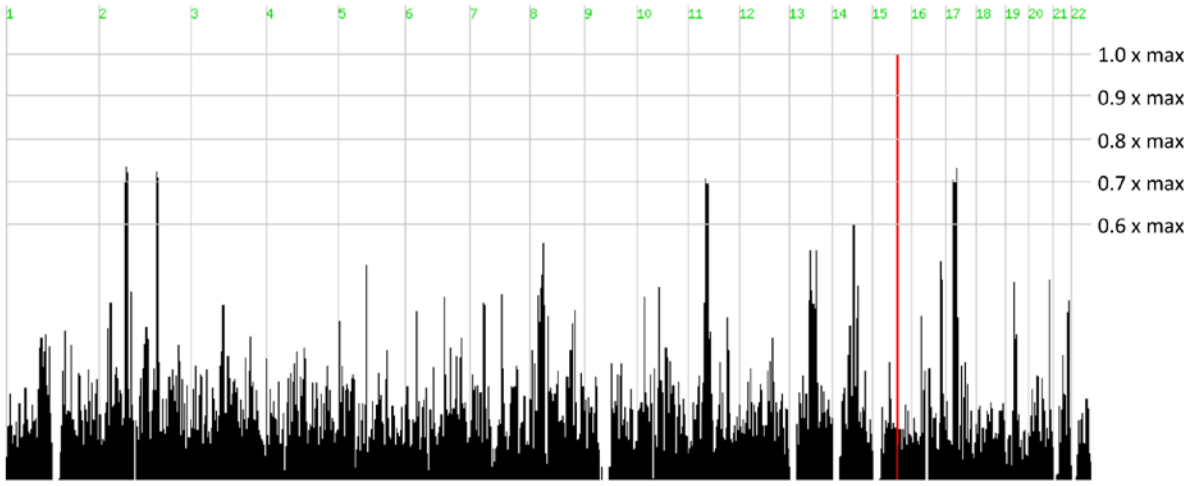


***Figure S4.*** **Autozygosity mapping of Family B** Three affected and two unaffected individuals were used for the analysis. The red bars depict the regions that were only homozygous in the patients and not in the unaffected family members at Chr15:63,594,231-68 726 159 (rs12910654-rs12915814). A *shared autozygous region* between Families A and B comprised an interval on Chr15:63,594,231-66,260,894 (rs12910654-rs333556) that contained 38 protein-coding genes.

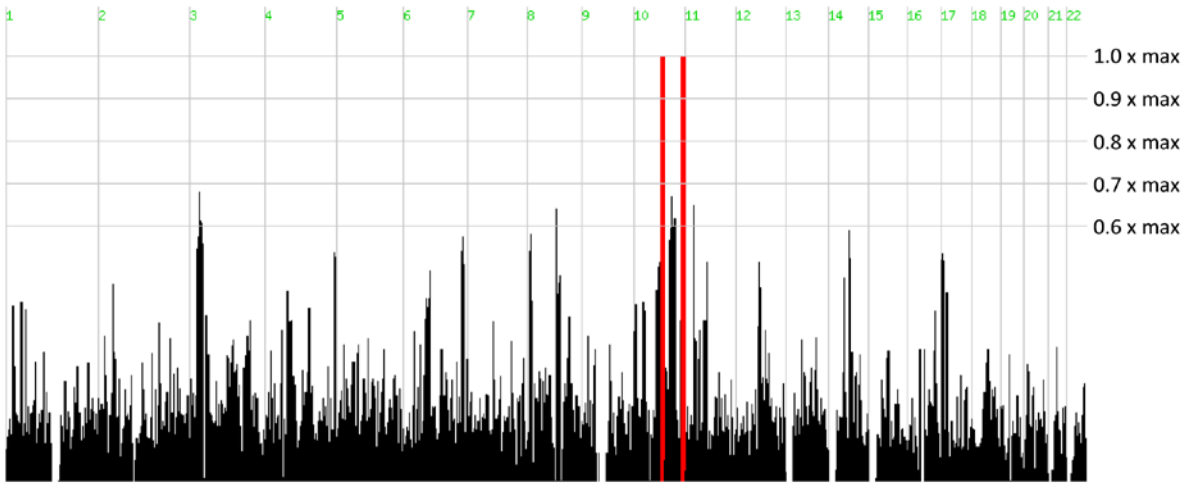


***Figure S5.*** **Autozygosity mapping of Family D** Two affected and one unaffected individual were used for the analysis. The red bars depict the regions that were only homozygous in the patients and not in the unaffected family member at Chr10:71,613,489-81,169,345 (rs2683563-rs10824752) and Chr10:124,114,432-135,422,505 (rs7905027-rs4498943) comprising 196 protein coding genes.

## In-situ hybridization of whole E17.5 mouse embryos

***Figure S6.*** **Comparison of in-situ intensities for *Trip4* antisense and sense probes.** In-situ hybridization of a parasagittal section of an E17.5 C57BL6/J embryo with a *Trip4* antisense probe (left) and the corresponding sense probe (right). Both DIG-labeled RNA-probes were generated from the same plasmid via transcription from the T3 promoter (antisense) or the T7 promoter (sense) of the pCR-Script plasmid. Due to the large size of the embryo single sub-images are stitched together to represent the entire embryo on a single image. Both images have been recorded with the identical illumination settings.

***Figure S7.*** **Comparison of in-situ intensities for *Ascc1* antisense and sense probes.** In-situ hybridization of a parasagittal section of an E17.5 C57BL6/J embryo with an *Ascc1* antisense probe (left) and the corresponding sense probe (right). Both DIG-labeled RNA-probes were generated from the same plasmid *via* transcription from the T3 promoter (antisense) or the T7 promoter (sense) of the pCR-Script plasmid. Due to the large size of the embryo single sub-images are stitched together to represent the entire embryo on a single image. Both images have been recorded with the identical illumination settings.

## Quantification of morpholino injection into zebrafish

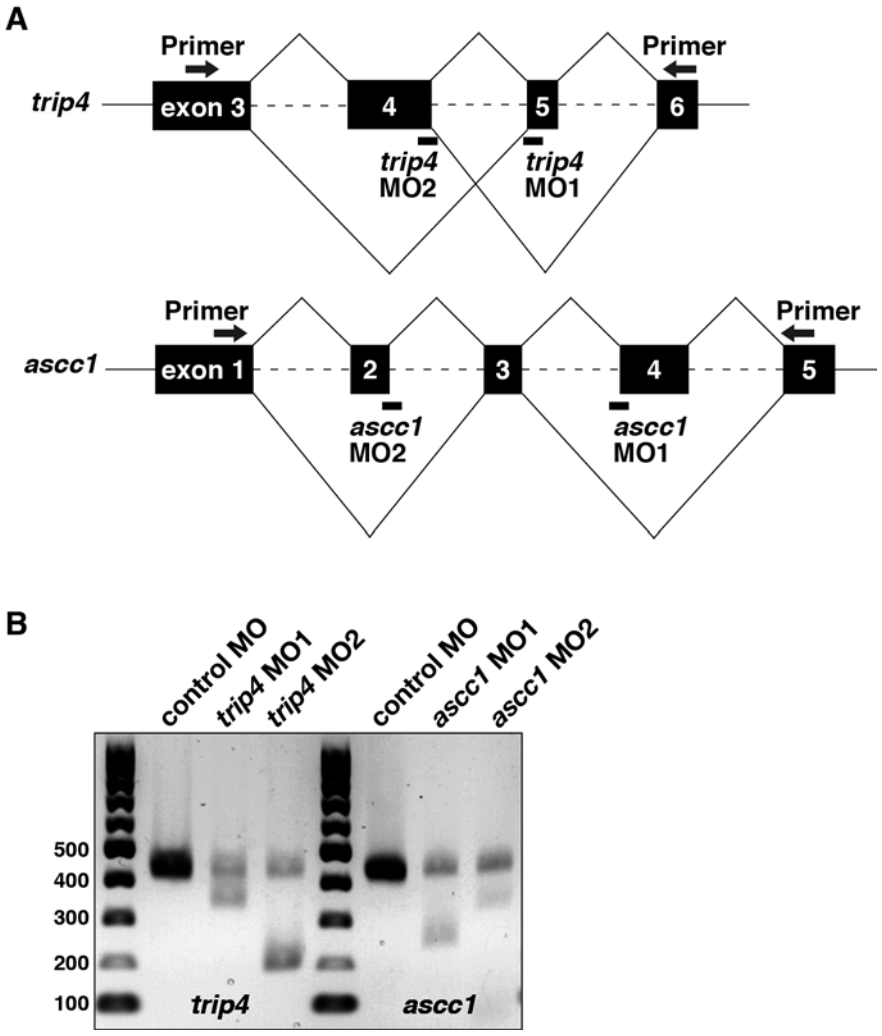


***Figure S8.*** **Morpholino mediated exon skipping in *ascc1* and *trip4* transcripts. (A)** Location of the MOs at the *trip4* and *ascc1* splice junctions, position of the oligonucleotide primers used for RT-PCR and exon skipping patterns. **(B)** Agarose gel electrophoresis of *trip4* and *ascc1* RT-PCR products in differently injected zebrafish embryos verifying exon skipping. The sizes of the skipped exons are: *trip4* MO1 = exon 5 (79 bp); *trip4* MO2 = exon 4 (219 bp); *ascc1* MO1 = exon 4 (180 bp); *ascc1* MO2 = exon 2 (100 bp). red = in-frame deletion, blue = out-of-frame deletion

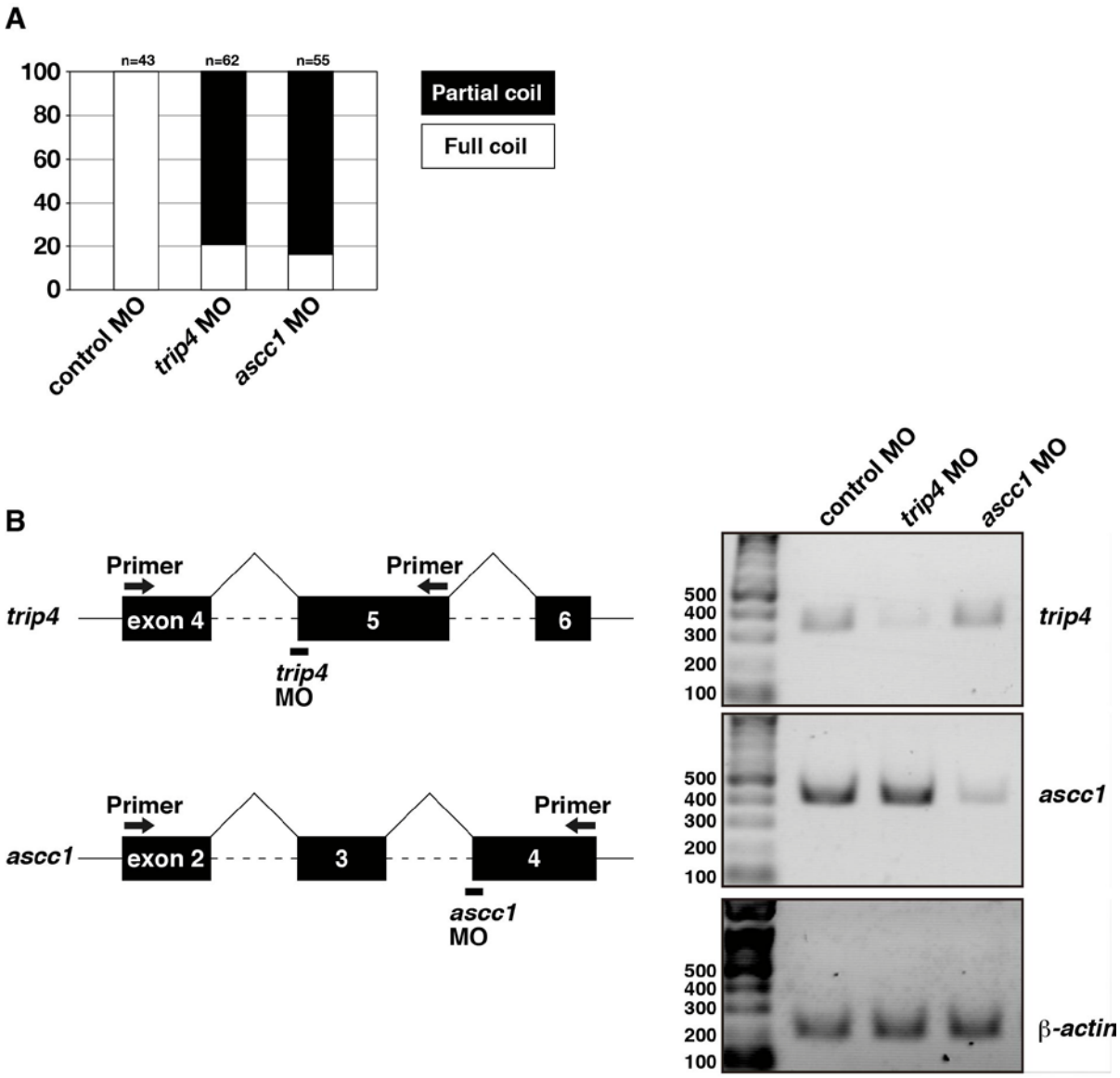


***Figure S9.*** **Morpholino mediated knockdown of *ascc1* and *trip4*. (A)** Effect of control, *trip4* and *ascc1* MO (5 ng each) mediated knockdown on the ability of the 30 hpf zebrafish embryos for "full coil" or "partial coil". **(B)** ***Left panel:*** Location of the MOs at *trip4* and *ascc1* splice junctions and position of the oligonucleotide primers used for RT-PCR. ***Right panels:*** Agarose gel electrophoresis of *trip4* and *ascc1* RT-PCR products in differently injected zebrafish embryos verifying the specific knockdown of the intended targets. β-actin mRNA was taken as reference.

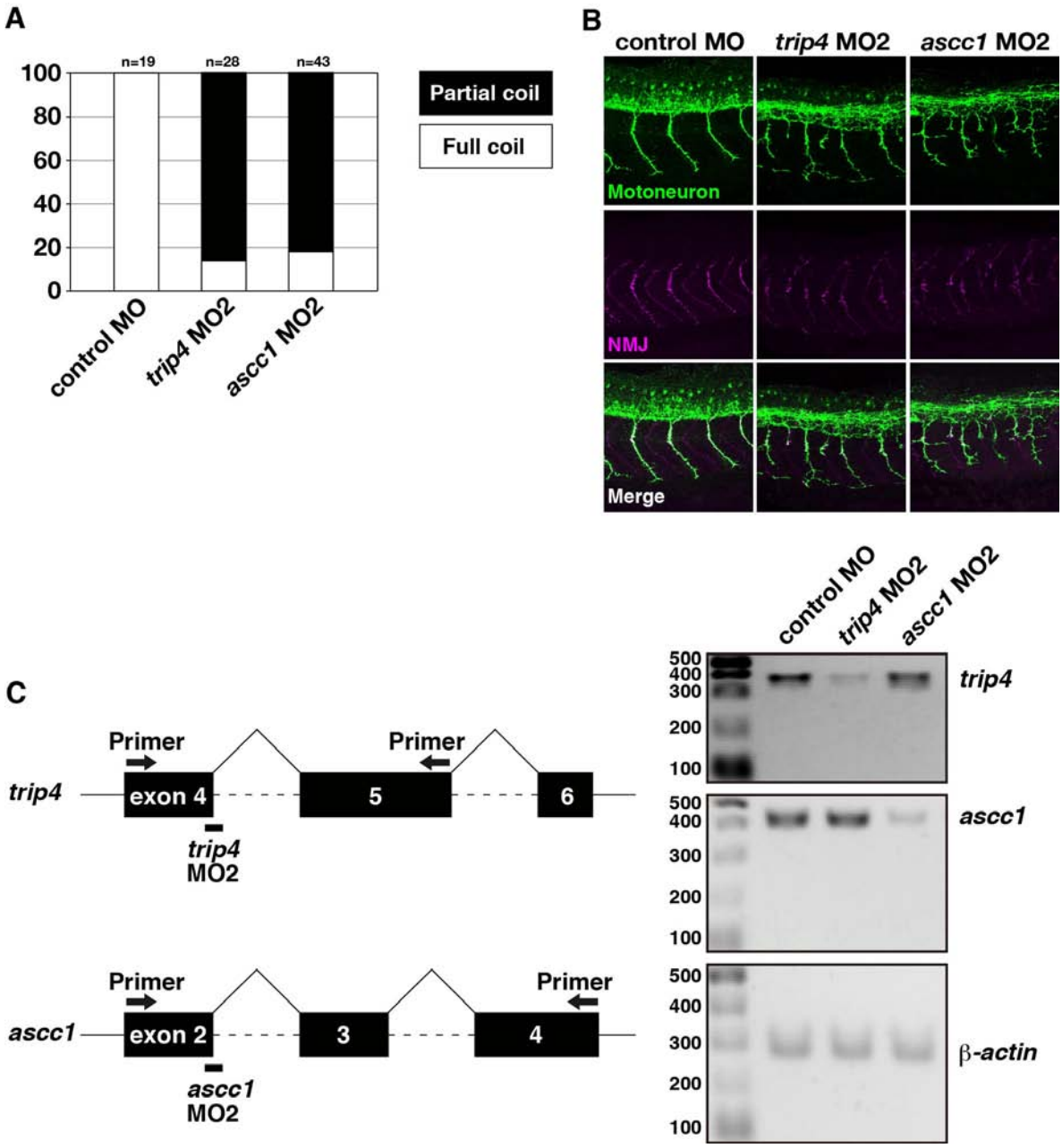


***Figure S10.*** **Use of alternative MO2 constructs for *trip4* and *ascc1* knockdown. (A)** Effect of control, *trip4* and *ascc1* MO2 (5 ng each) mediated knockdown on the ability of the 30 hpf zebrafish embryos for "full coil" or "partial coil". **(B)** The alternative *trip4* and *ascc1* MO2s have the same specificity to generate the morphologic abnormalities of the α-motoneuron and the neuromuscular junction as the respective MOs (see Figure 3C for comparison), hence verifying the specificity of the effect. **(C)** ***Left panel:*** Location of the MO2s at *trip4* and *ascc1* splice junctions and position of the oligonucleotide primers used for RT-PCR. ***Right panels:*** Agarose gel electrophoresis of *trip4* and *ascc1* RT-PCR products in differently injected zebrafish embryos verifying the specific knockdown of the intended targets. β-actin mRNA was taken as reference.

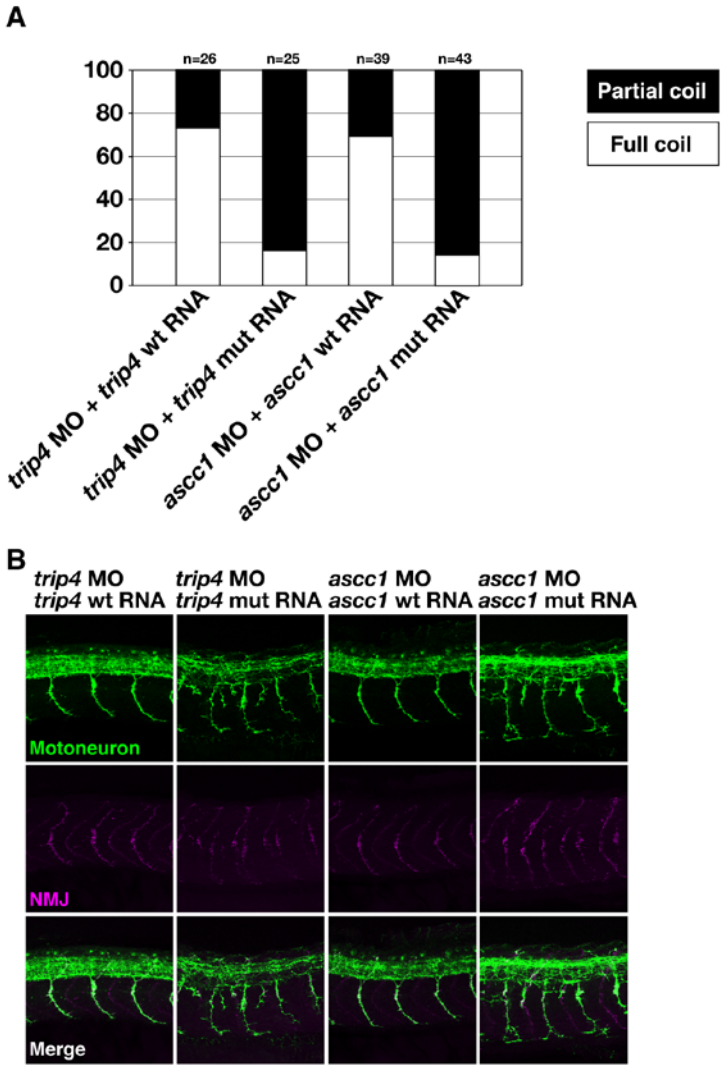


***Figure S11.*** **Rescue of MO-knockdown with wildtype and mutant mRNAs.** Simultaneous injection of morpholinos and rescue mRNA into zebrafish larvae rescues **(A)** the clinical phenotype ("coiling" behavior) and **(B)** the morphological abnormalities of the α-motoneuron projections only if wildtype mRNA is injected and not by injection of mRNA carrying the zebrafish equivalents of the patient mutations.

## Expression of SRF responsive genes after serum challenge

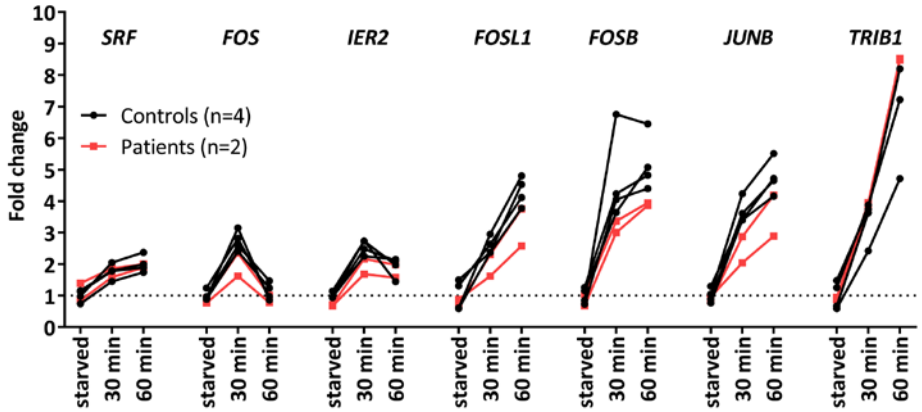


***Figure S12.*** **Expression of known SRF responsive target genes after serum challenge.** Human skin fibroblasts were grown in DMEM + 15% FBS, then serum starved for 24 hours and re-challenged with 15% FBS for 30 and 60 minutes. The lines depict the fold change of gene expression from baseline (serum starvation). The red lines depict the patients, the black lines the controls. There was no significant and persistent difference in the response of the SRF downstream target genes.

## Subcellular location of the ASC-1 complex and of the CSRP1 protein

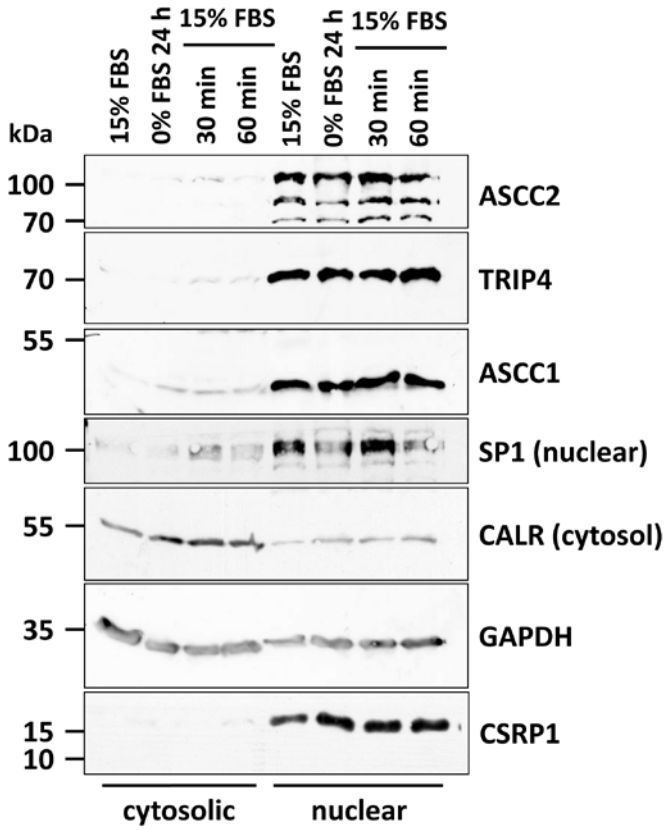


***Figure S13.*** **Subcellular localization of the ASC-1 complex and of the CSRP1 protein after serum starvation and challenge.** The members of the ASC-1 complex TRIP4, ASCC1, and ASCC2 as well as the CSRP1 protein remain in the nucleus independently of the status of serum depletion or challenge of fibroblasts. As control for the subcellular fractionation, transcription factor SP1, a nuclear maker protein, is enriched in the nuclear fraction and the Calreticulin protein (CALR), a marker protein for the endoplasmatic reticulum (ER) is depleted in the nuclear fraction.

## Multiple species alignment of TRIP4 and ASCC1 amino acid sequences

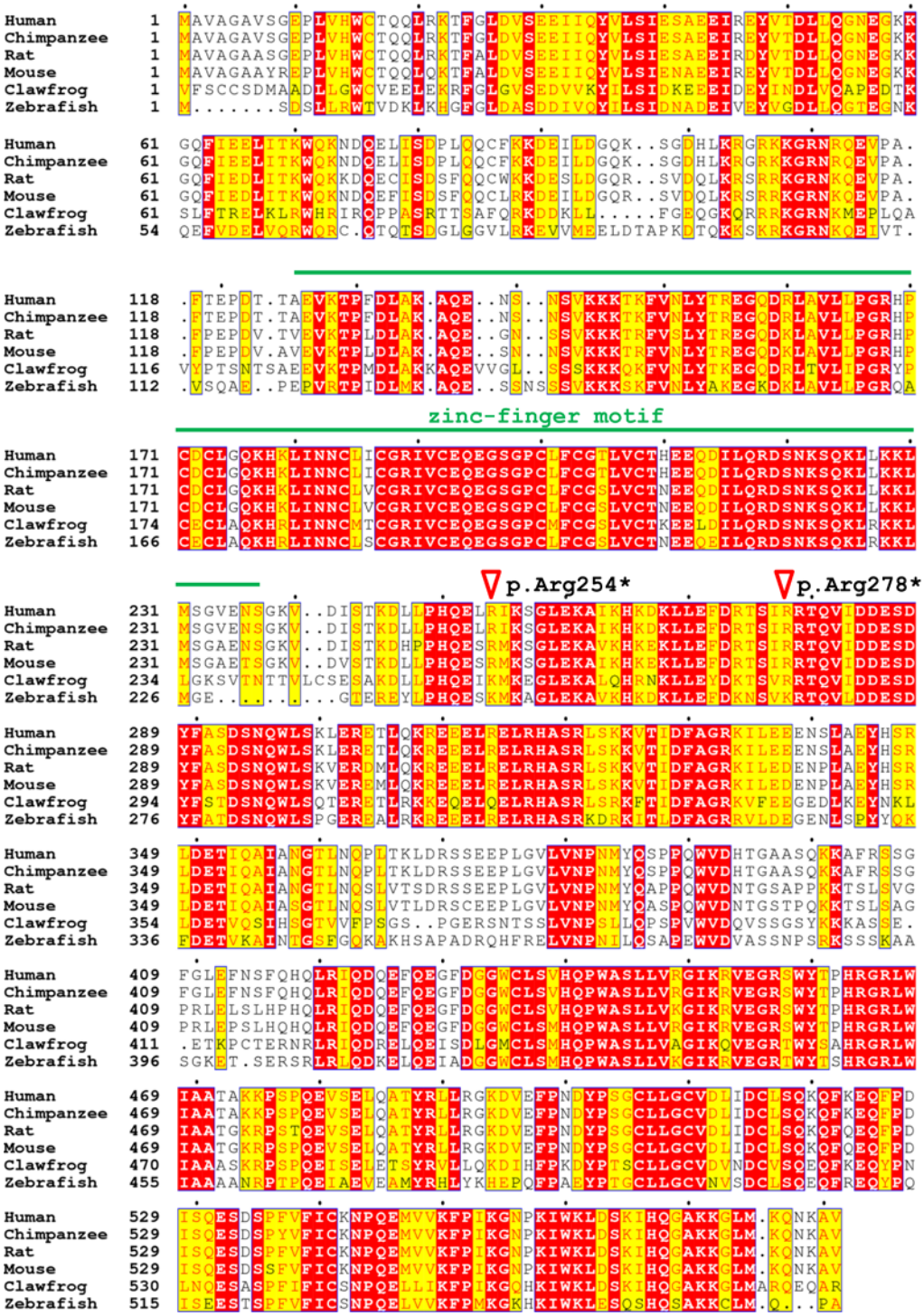


***Figure S14.*** **Multiple species alignment of TRIP4** Red boxes depict identical, yellow boxes similar amino acids. The zinc-finger motif (aa125-237) is depicted by a green line. The positions of the two nonsense mutations are depicted by a red triangle. The Ensembl accession number for the amino acid sequences are: Human [ENSP00000261884], Chimpanzee [ENSPTRP00000012241], Rat [ENSRNOP00000021863], Mouse [ENSMUSP00000112385], Clawfrog [ENSXETP00000023326], Zebrafish [ENSDARP00000107782]

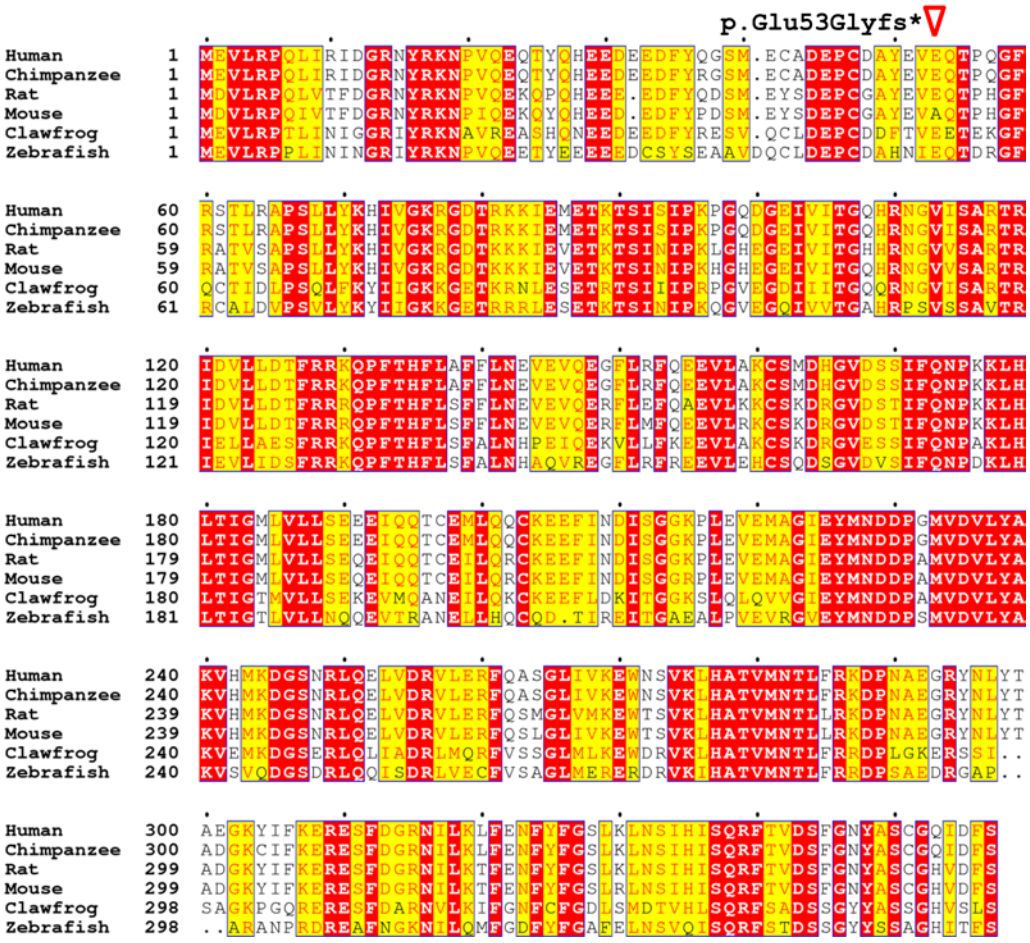


***Figure S15.*** **Multiple species alignment of ASCC1** Red boxes depict identical, yellow boxes similar amino acids. The position of the frameshift mutation is depicted by a red triangle. The Ensembl/GenBank accession number for the amino acid sequences are: Human [ENSP00000320810], Chimpanzee [ENSPTRP00000004528], Rat [ENSRNOP00000000701], Mouse [ENSMUSP00000052351], Clawfrog [ENSXETP00000013525], Zebrafish [NP_001017610]. The multiple amino acid sequence alignment was performed with T-Coffee and the coloring /printout with ESPript.[1]

## Co-immunoprecipitation with antibodies against three subunits of the ASC-1 complex

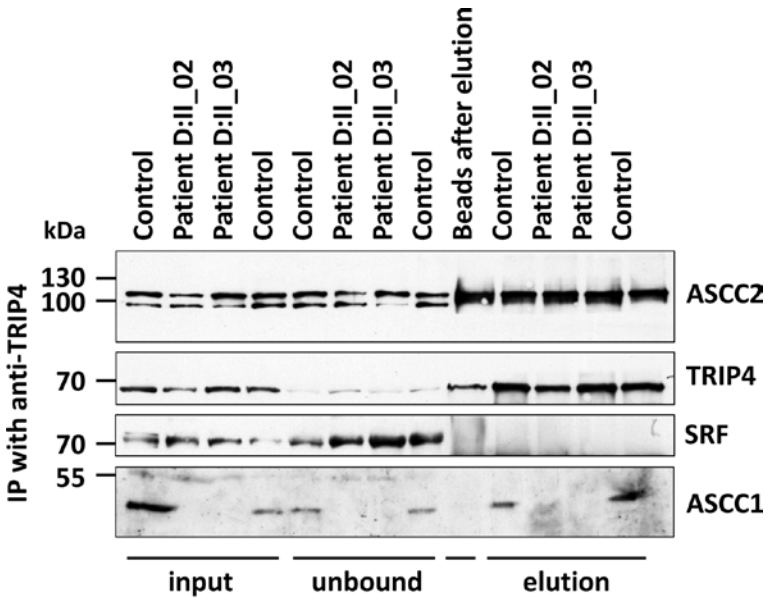


***Figure S16.*** **Immunoprecipitation with an anti-TRIP4 antibody.** Co-precipitation with TRIP4 can be seen for ASCC1, and ASCC2. ASCC1 is only seen controls, but not in both patients. Hence, even in the absence of the ASCC1 subunit the remaining ASC-1 protein complex seems to be formed. SRF is not co-precipitated TRIP4 (or the ASC-1 complex) and can only be detected in the unbound flow-through.

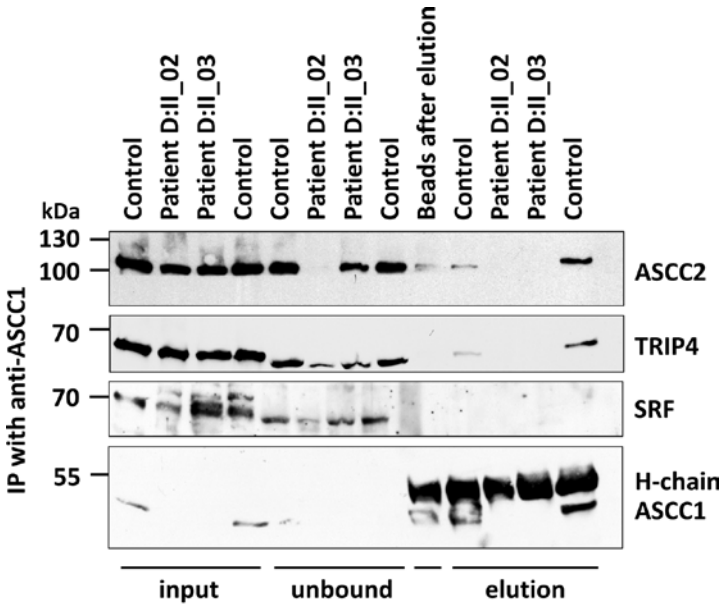


***Figure S17.*** **Immunoprecipitation with an anti-ASCC1 antibody.** Co-precipitation with ASCC1 can be seen for TRIP4 and ASCC2 only in the controls, not in the patients. SRF is not co-precipitated ASCC1 (or the ASC-1 complex) and can only be detected in the unbound flow-through.

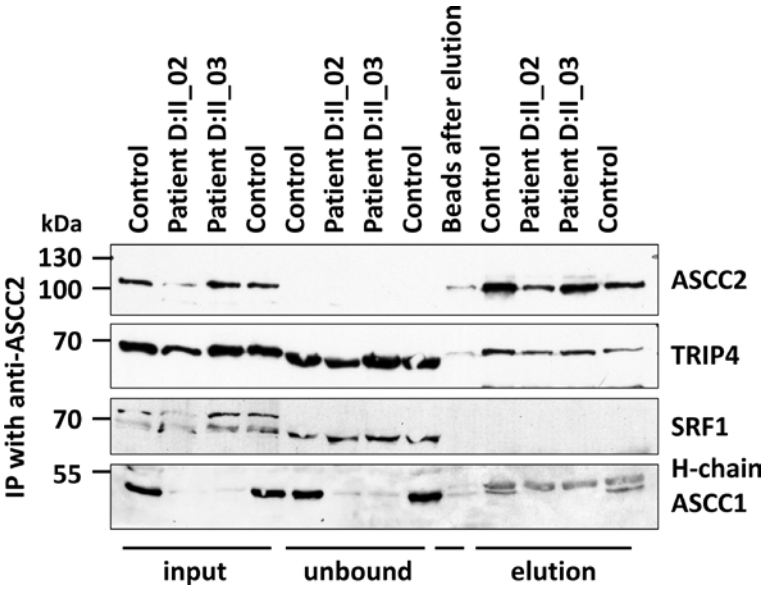


***Figure S18.*** **Immunoprecipitation with an anti-ASCC2 antibody. (A)** Co-precipitation with ASSC2 can be seen for TRIP4 and ASCC1 only in the controls, not in the patients. SRF is not co-precipitated ASCC2 (or the ASC-1 complex) and can only be detected in the unbound flow-through.

## HCD spectra of peptides from interacting proteins

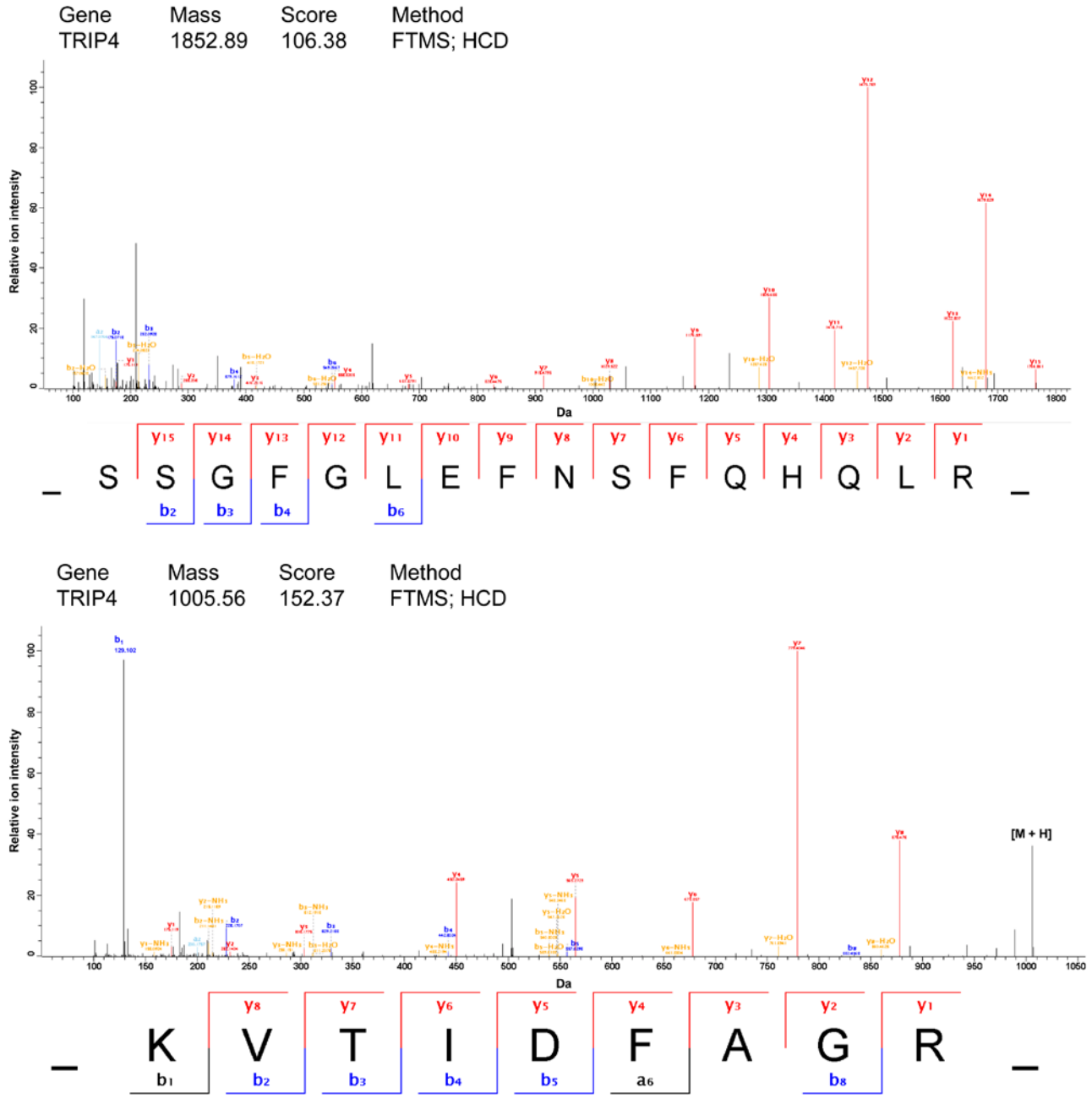


***Figure S19.*** **MS spectra of two identified TRIP4 peptides.** The b- and y- ion series of the Higher-energy collisional dissociation (HCD) spectrum.

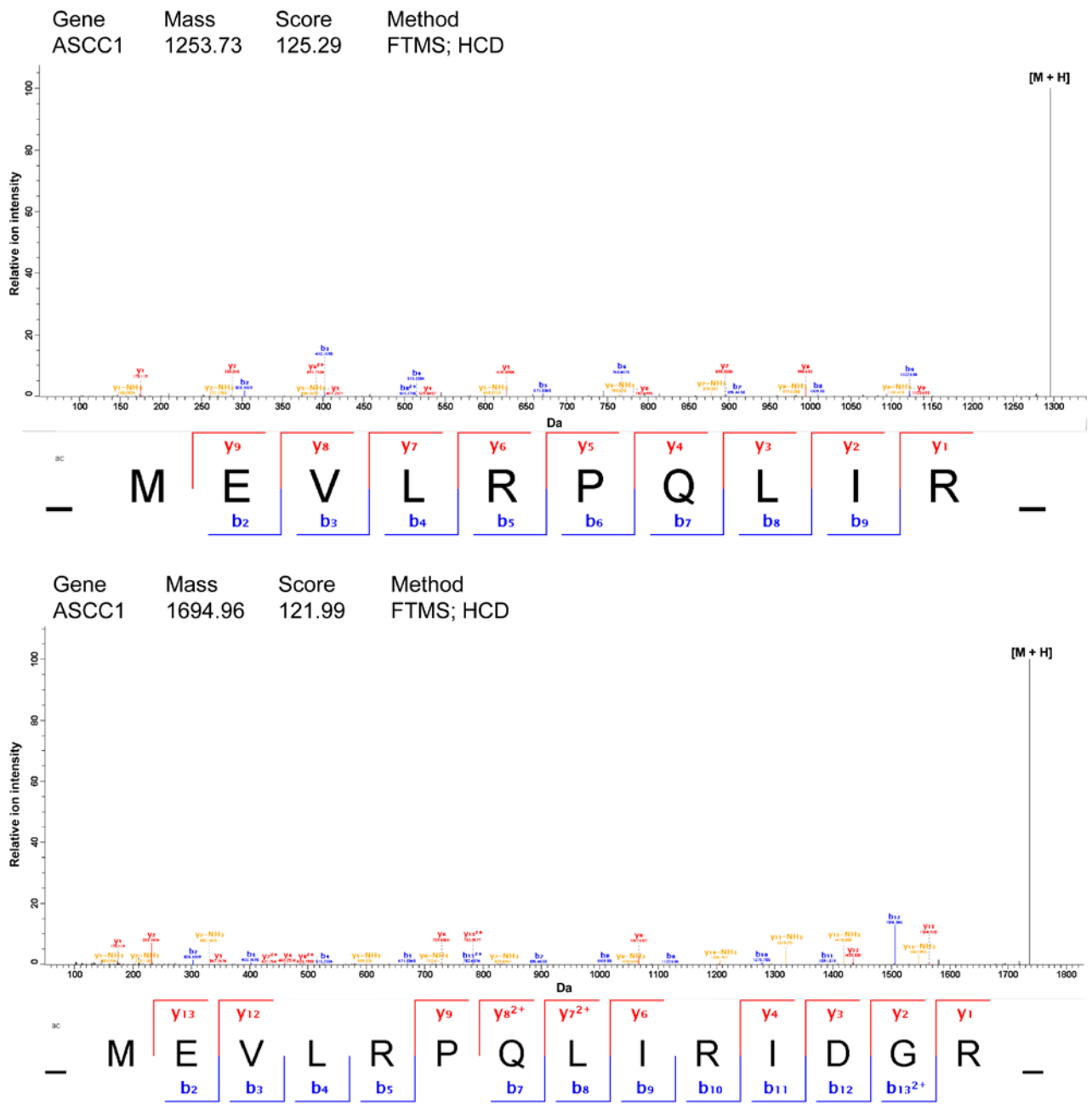


***Figure S20.*** **MS spectra of two identified ASCC1 peptides.** The b- and y- ion series of the Higher-energy collisional dissociation (HCD) spectrum.

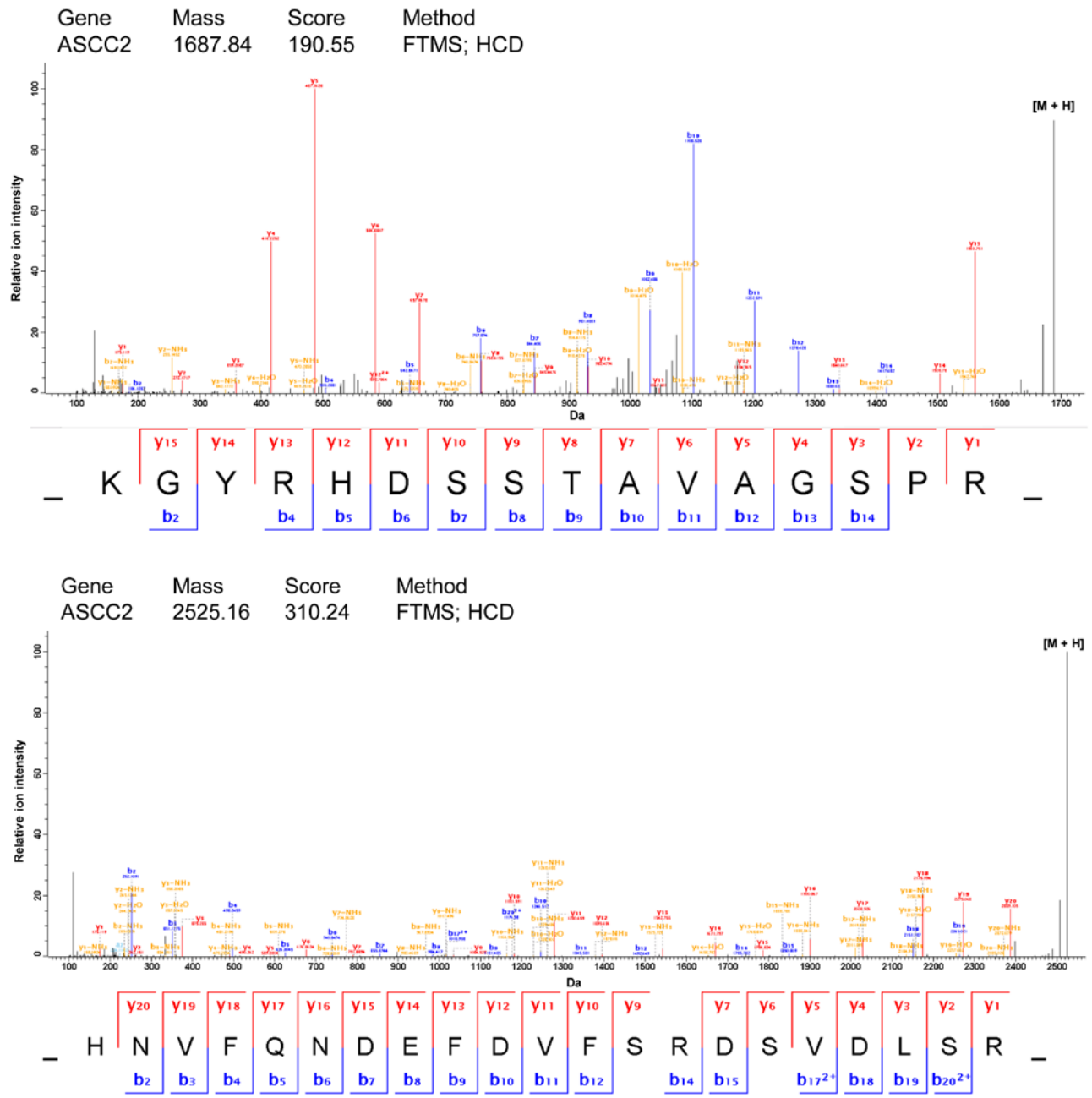


***Figure S21.*** **MS spectra of two identified ASCC2 peptides.** The b- and y- ion series of the Higher-energy collisional dissociation (HCD) spectrum.

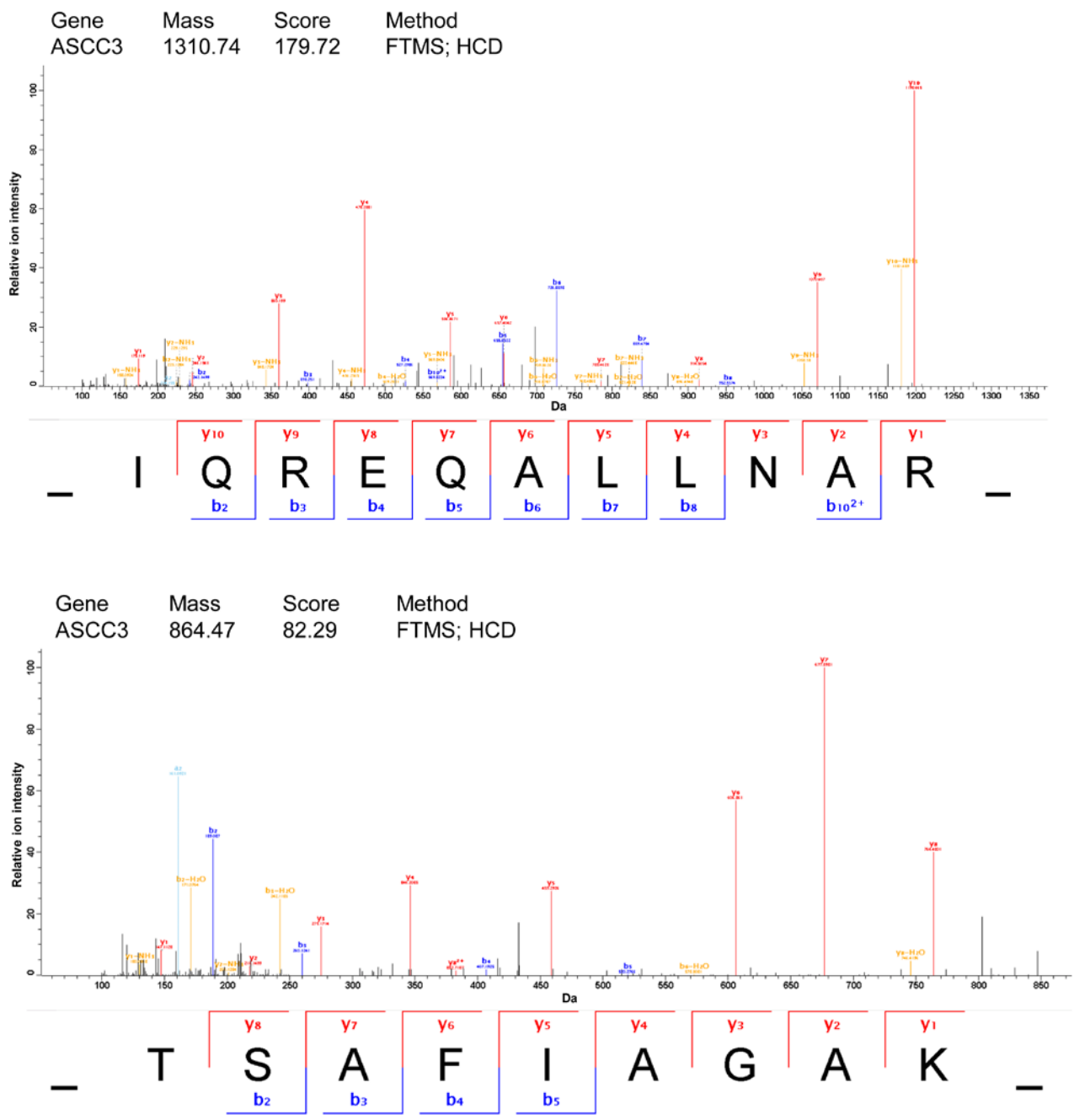


***Figure S22.*** **MS spectra of two identified ASCC3 peptides.** The b- and y- ion series of the Higher-energy collisional dissociation (HCD) spectrum.

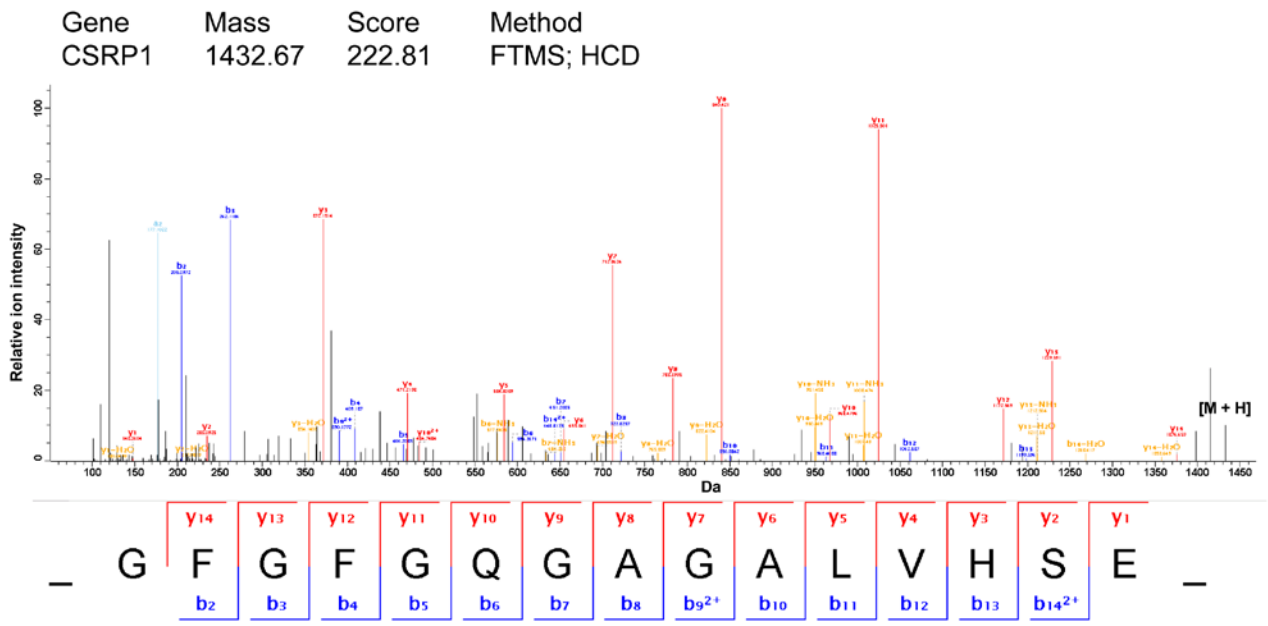


***Figure S23.*** **MS spectrum of one identified CSRP1 peptide.** The b- and y- ion series of the Higher-energy collisional dissociation (HCD) spectrum.

## Morphometric analysis of the sural nerve

***Table S1.*** **Fiber density of myelinated fibers in patients and control**

| Patient | Median | 10th percentile | 90th percentile |
|---|---|---|---|
| **Control** | 22,059 $mm^2$ | 18,971 $mm^2$ | 25,111 $mm^2$ |
| **B:II_05 (*TRIP4*)** | 22,752 $mm^2$ | 21,781 $mm^2$ | 23,169 $mm^2$ |
| **D:II_02 (*ASCC1*)** | 21,781 $mm^2$ | 16,509 $mm^2$ | 28,857 $mm^2$ |

## Coverage details of the exome sequencing

***Table S2.*** **Coverage details of three WES datasets**

| Individual | Mean coverage [fold] | Coverage per base of captured exons | | | 100 bp paired-end fragments [n] |
|---|---|---|---|---|---|
| | | >3x [%] | >10x [%] | >20x [%] | |
| **B.II_01** | 175.99 | 99.8 | 99.4 | 98.7 | 77.3 Mio |
| **D.II_02** | 112.91 | 99.5 | 98.7 | 97.0 | 53.2 Mio |
| **D.II_03** | 230.12 | 99.8 | 99.5 | 98.9 | 106.1 Mio |

## Quantification of morpholino injection into zebrafish

***Table S3.*** **Quantification of the "coiling" behavior of morphants and controls**

| **Morpholino [amount injected]** | | **"partial coil"/total number of examined embryos (p-value in comparison to *bactin* MO injection; $\chi^2$-test)** | **Affected embryos [%]** |
|---|---|---|---|
| Control [5 ng] | | 0/43 ($p$<0.001) | 0 |
| *trip4* MO [5 ng] | | 49/62 ($p$<0.001) | 79 |
| *ascc1* MO [5 ng] | | 46/55 ($p$<0.001) | 84 |
| **Morpholino [amount injected]** | **Primer set** | **Specific/bactin RT-PCR band density [mean±SD; t-test]** | **N** |
| *trip4* MO [5 ng] | *trip4* | 0.15±0.09 ($p$<0.01) | 4 |
| *trip4* MO [5 ng] | *ascc1* | 0.92±0.07 ($p$>0.05) | 4 |
| *ascc1* MO [5 ng] | *trip4* | 1.03±0.31 ($p$>0.80) | 4 |
| *ascc1* MO [5 ng] | *ascc1* | 0.17±0.09 ($p$<0.01) | 4 |

***Table S4.*** **Quantification of the "coiling" behavior using an alternative morpholino**

| **Morpholino [amount injected]** | | **"partial coil"/total number of examined embryos (p-value in comparison to *bactin* MO injection; $\chi^2$-test)** | **Affected embryos [%]** |
|---|---|---|---|
| Control [5 ng] | | 0 /19 ($p$<0.001) | 0 |
| *trip4* MO2 [5 ng] | | 24/28 ($p$<0.001) | 86 |
| *ascc1* MO2 [5 ng] | | 35/43 ($p$<0.001) | 81 |
| **Morpholino [amount injected]** | **Primer set** | **Specific/bactin RT-PCR band density [mean±SD; t-test]** | **N** |
| *trip4* MO2 [5 ng] | *trip4* | 0.19±0.11 ($p$<0.001) | 4 |
| *trip4* MO2 [5 ng] | *ascc1* | 1.00±0.09 ($p$>0.9) | 4 |
| *ascc1* MO2 [5 ng] | *trip4* | 0.92±0.09 ($p$>0.15) | 4 |
| *ascc1* MO2 [5 ng] | *ascc1* | 0.14±0.10 ($p$<0.001) | 4 |

***Table S5.*** **Quantification of the density of neuromuscular junctions**

| **Morpholino** | **Amount injected [ng]** | **Cumulative relative density of the neuromuscular junction in comparison to CTRL MO [± SD]** |
|---|---|---|
| CTRL MO | 5 | 1.00±0.26 (n=4) |
| *ascc1* MO | 5 | 0.61±0.12 (n=4, p<0.05) |
| *trip4* MO | 5 | 0.56±0.18 (n=4, p<0.05) |

## Quantification of gene expression in patient and control fibroblasts

***Table S6.*** **Differentially regulated genes in *ASCC1* mutant versus control skin fibroblasts**
(The PubMed link can be directly clicked and connects to the PubMed abstract of the cited article)

| Gene symbol (HGNC) | Fold change | FDR (BH) | Gene name | Gene Ontology (GO) annotation | Direct link to PubMed |
|---|---|---|---|---|---|
| **Genes in nervous system development (DOWN-REGULATED)** | | | | | |
| ***SERPINF1*** | **-5.7** | 0.0045 | Serpin peptidase inhibitor, clade F (alpha-2 antiplasmin, pigment epithelium derived factor), member 1 | positive regulation of neuron projection development | PMID:23825416 |
| | | | | neuronal cell body | PMID:10411342 |
| | | | | negative regulation of neuron death | PMID:22410737 |
| | | | | positive regulator of neurogenesis | PMID:8226833 |
| ***GSTM3*** | **-2.1** | 0.0045 | Glutathione S-transferase mu 3 (brain) | establishment of blood-nerve barrier | PMID:2345169 |
| ***DAB1*** | **-6.4** | 0.0045 | Dab, reelin signal transducer, homolog 1 (Drosophila) | lateral motor column neuron migration | PMID:20711475 |
| | | | | positive regulation of neuron differentiation | PMID:18848628 |
| | | | | neuron migration | PMID:15703280, PMID:15091337, PMID:11226314, PMID:12882964, PMID:8875886 |
| | | | | neuron projection | PMID:14961563 |
| | | | | neuronal cell body | PMID:14961563 |
| ***LAMA4*** | **-2.8** | 0.0045 | Laminin, alpha 4 | muscle attachment | PMID:22859503 |
| ***FHOD3*** | **-2.1** | 0.0045 | Formin homology 2 domain containing 3 | sarcomere organization | PMID:19706596, PMID:22509354 |
| ***CRLF1*** | **-2.2** | 0.0045 | Cytokine receptor-like factor 1 | negative regulation of neuron apoptotic process | PMID:10966616 |
| | | | | negative regulation of motor neuron apoptotic process | PMID:14523086 |
| ***SEMA3D*** | **-2.3** | 0.0045 | Semaphorin 3D | axon guidance | PMID:15456815, PMID:17251263 |
| | | | | peripheral nervous system development | PMID:16280593 |
| | | | | retinal ganglion cell axon guidance | PMID:14724229, PMID:16467361 |
| | | | | Neural crest development | PMID:16971468 |
| | | | | regulation of axon extension | PMID:16280593 |
| | | | | neural crest cell differentiation | PMID:16860789, PMID:16971468 |

| | | | | | |
|---|---|---|---|---|---|
| ***SEMA3A*** | **-5.1** | 0.0045 | Semaphorin 3A | retinal ganglion cell axon guidance | PMID:16467361, PMID:14724229 |
| | | | | neural crest cell development | PMID:16971468 |
| | | | | regulation of axon extension | PMID:16280593 |
| | | | | pathway involved in axon guidance | PMID:18804103 |
| | | | | axogenesis involved in innervation | PMID:22790009 |
| ***PPAP2B*** | **-1.9** | 0.0045 | Phosphatidic acid phosphatase type 2B | Bergmann glial cell differentiation | PMID:21319224 |
| | | | | ossification | PMID:12933688 |
| | | | | response to vitamin D | PMID:11702003 |
| ***CRABP2*** | **-1.6** | 0.0078 | Cellular retinoic acid binding protein 2 | embryonic forelimb morphogenesis | PMID:7720575 |
| | | | | hindbrain morphogenesis | PMID:22619388 |
| | | | | positive regulation of collateral sprouting | PMID:18052984 |
| ***FZD4*** | **-2.1** | 0.0045 | Frizzled class receptor 4 | cerebellum vasculature morphogenesis | PMID:15035989, PMID:12230512 |
| ***ASPA*** | **-2.7** | 0.0078 | Aspartoacylase | positive regulation of oligodendrocyte differentiation | PMID:16634055 |
| ***NOV*** | **-2.6** | 0.0078 | Nephroblastoma overexpressed | axon development | PMID:19286457 |
| | | | | neuronal cell development | PMID:19286457 |
| | | | | dendrite formation | PMID:19286457 |
| **Genes in nervous system development (UP-REGULATED)** | | | | | |
| ***HAPLN1*** | **+6.7** | 0.0045 | Hyaluronan and proteoglycan link protein | Suppression of neuronal plasticity | PMID:20566484 |
| | | | | Memory function | PMID:23595763 |
| | | | | Extracellular matrix | PMID:23595763 |
| ***EDIL3*** | **+3.1** | 0.0045 | EGF-like repeats and discoidin I-like domains 3 | Neural plate development | PMID:20823067 |
| ***NTN4*** | **+3.1** | 0.0045 | Netrin 4 | Neuron remodeling | PMID:11038171 |
| ***ITGA*** | **+1.7** | 0.0045 | Integrin alpha-3 | Neuron migration | PMID:15091337 |
| | | | | Excitatory synapse | PMID:23595732 |
| | | | | Regulation of neuron projection development | PMID:2223092 |
| ***CDH13*** | **+2.0** | 0.0045 | Cadherin-13 | Negative regulation of neuron projection | PMID:10737605 |
| | | | | Negative regulation of cell proliferation | PMID:10737605 |

| Gene symbol (HGNC) | Fold change | FDR (BH) | Gene name | Gene Ontology (GO) annotation | Direct link to PubMed |
|---|---|---|---|---|---|
| **Genes in bone development (DOWN-REGULATED)** | | | | | |
| ***TNFRSF11B*** | **-4.8** | 0.0045 | Tumor necrosis factor receptor superfamily, member 11b | negative regulation of odontogenesis of dentin-containing tooth | PMID:16283633 PMID:14981127 |
| | | | | negative regulation of bone resorption | PMID:11839361 PMID:16912914 |
| | | | | skeletal system development | PMID:9108485 |
| ***FAM20A*** | **-1.9** | 0.0045 | Family with sequence similarity 20, member A | tooth eruption | PMID:23434854 PMID:23468644 PMID:23697977 |
| | | | | calcium ion homeostasis | PMID:23434854 |
| ***RASSF2*** | **-2.5** | 0.0078 | Ras association (RalGDS/AF-6) domain family member 2 | bone remodeling | PMID:22227519 |
| | | | | ossification | PMID:22227519 |
| | | | | regulation of osteoblast differentiation | PMID:22227519 |
| | | | | regulation of osteoclast differentiation | PMID:22227519 |
| | | | | skeletal system development | PMID:22227519 |
| ***TSHZ2*** | **-2.2** | 0.0045 | Teashirt zinc finger homeobox 2 | embryonic cranial skeleton morphogenesis | PMID:23559552 |
| ***STC1*** | **-3.0** | 0.0078 | Stanniocalcin 1 | positive regulation of calcium ion import | PMID:17032941 |
| ***DPT*** | **-2.5** | 0.0045 | Dermatopontin | collagen fibril organization | PMID:16877395 |

## Mass spectrometric analysis of peptides from immunoprecipitations

***Table S7.*** **Mass spectrometric analysis of peptides from immunoprecipitations (TableS7.xlsx)**

Immunoprecipitated samples were boiled at 95°C for 5 min, reduced in 50 mM DTT and alkylated with a final concentration of 5.5 mM chloroacetamide for 30 min. Proteins were digested by 250 ng of trypsin overnight at 37°C and desalted with C18 columns. Each sample fraction was dissolved in 2 µL of 5% ACN and 2% FA for subsequent MS analysis. LC–MS/MS was carried out by nanoflow reverse-phase liquid chromatography (Dionex Ultimate 3000, Thermo Scientific; Waltham, MA) coupled online to a Q-Exactive Plus Orbitrap mass spectrometer (Thermo Scientific). Briefly, LC separation was performed using a PicoFrit analytical column (75 µm ID × 25 cm long, 15 µm Tip ID (New Objectives, Woburn, MA)) in -house packed with 3 µm C18 resin (Reprosil-AQ Pur, Dr. Maisch, Germany). Peptides were eluted using a gradient from 3.8 to 98% solvent B over 46 min at a flow rate of 300 nL/min (solvent A: 0.1% formic acid in water; solvent B: 80% acetonitrile and 0.08% formic acid). Three kilovolts were applied for nanoelectrospray generation. A cycle of one full FT scan mass spectrum (300–1700 m/z, resolution of 35000 at m/z 200) was followed by 12 data-dependent MS/MS scans with a normalized collision energy of 25 eV. Raw MS data were processed with MaxQuant software (version 1.5.0.0) and searched against the human proteome database UniProtKB with 88,717 entries, released 2014-11. A false discovery rate (FDR) of 0.01 for proteins and peptides and a minimum peptide length of 7 amino acids were required. A maximum of two missed cleavages was allowed for the tryptic digest. Cysteine carbamidomethylation was set as fixed modification, whereas N-terminal protein acetylation and methionine oxidation were set as variable modifications.

## Oligonucleotides used for sequencing, cloning, in vitro mutagenesis and morpholino mediated knockdown

***Table S8.*** **Oligonucleotides used for molecular genetics experiments**

| Gene | Exon | Forward | Reverse | Product size [bp] |
|---|---|---|---|---|
| **Sequencing of genomic DNA** | | | | |
| *ASCC1* | Ex 3 | 5-CCCAATTCAGACCTGCATAA-3 | 5-TTGATCCTACAATACACAGGACA-3 | 296 |
| *ASCC1* | Ex 4 | 5-AGCGGTTGACAGCTGAGG-3 | 5-TCAAGCACTGCAATAAGTATGGA-3 | 275 |
| *ASCC1* | Ex 5 | 5-TCTCTTGTCACAAAGGATTTAAACA-3 | 5-CCCATAGCTAGAACCCCACA-3 | 299 |
| *ASCC1* | Ex 6 | 5-TCAGAACTGCTTTAGCTCCTCA-3 | 5-TTGGTGGGGGAAGAAGTTTA-3 | 390 |
| *ASCC1* | Ex 7 | 5-TGGGCTGAGTTTCTTGTTTT-3 | 5-CTGAGAATTACTCACATACCAAAAAG-3 | 249 |
| *ASCC1* | Ex 8 | 5-TTTTGAAATTAGAAGGGCAATTAGA-3 | 5-TCAAAGAAAAGGAATCAAAATGAA-3 | 381 |
| *ASCC1* | Ex 9 | 5-GCAGGGCTTTGTATGGTGAT-3 | 5-TTGCCCACCTCTACTATGCTC-3 | 395 |
| *ASCC1* | Ex 10 | 5-TCATTATGCCACTTTCCAGGT-3 | 5-TGAAGAAATATACGGAGAACTACTTG-3 | 298 |
| *ASCC1* | Ex 11 | 5-GGGATTGTTGTGGTTTGGTG-3 | 5-CCCTGCTTGGCAATTAAAAC-3 | 300 |
| **Sequencing of genomic DNA** | | | | |
| *TRIP4* | Ex 1 | 5-GGGATCTGCACTGGAGGC-3 | 5-GCACATCCCAGAGCTCCTT-3 | 289 |
| *TRIP4* | Ex 2 | 5-CTCTGTTAAGATTACTGAGAAACAGTG-3 | 5-AGCCTGCCCACTTACCAATA-3 | 291 |
| *TRIP4* | Ex 3 | 5-TTCACCAGGAATCCTCTTATCAA-3 | 5-TCACTTCCTCTTCTCCAATAGTCA-3 | 248 |
| *TRIP4* | Ex 4 | 5-GGAGCATTTTCTCCCTTGAC-3 | 5-AGATCTGACTGGCTCTGCGT-3 | 352 |
| *TRIP4* | Ex 5 | 5-GCAATATAATTTAACTGTTGGATCAC-3 | 5-ACAAGGTACCCATCATCCCA-3 | 178 |
| *TRIP4* | Ex 6 | 5-TTGTTCTTTGTTGCACACTGG-3 | 5-ATGGCCAGAATCTGTGGACT-3 | 267 |
| *TRIP4* | Ex 7 | 5-AATCGGTCCTTATTTGTCAACAG-3 | 5-GACCCTTTCTAGTGCTGCTCA-3 | 298 |
| *TRIP4* | Ex 8 | 5-TGTTGGTGGTAAGCATTCTGAG-3 | 5-AAATTGGGGCCAAACTTCTT-3 | 244 |
| *TRIP4* | Ex 9 | 5-ACCTACCCCAGATTCTTGCC-3 | 5-TCTAAGATCTTCCACTGCCCA-3 | 285 |
| *TRIP4* | Ex 10 | 5-TGGGATATTCCAGGAAACTAGA-3 | 5-AACGTCAATGACTTCTCTCCA-3 | 241 |
| *TRIP4* | Ex 11 | 5-TCCTGAGTTCCAAGATCACAAA-3 | 5-ATGGCGAAACCCTGTCTCTA-3 | 199 |
| *TRIP4* | Ex 12 | 5-GCTTGTCCCAACTATCCTGAA-3 | 5-TCCCCATTCCTTACTACTGCAC-3 | 204 |
| *TRIP4* | Ex 13 | 5-TAACCAGAAGACCTGGGAGG-3 | 5-TTTCCAACTTGGTCCAATCTC-3 | 445 |

| | | | | |
|---|---|---|---|---|
| **Tailed primers for the cloning of the in-situ hybridization probes** | | | | |
| *Trip4* | *Not*I-*Sal*I | 5-GGAGGAGCGGCCGCCGTACCGGGAGCCGCTAGTA-3 (*Not*I site underlined) | 5-GGAGGAGTCGACCTTCTGGCCCAGGCAATCAC-3 (*Sal*I site underlined) | 512 |
| *Ascc1* | *Not*I-*Sal*I | 5-GGAGGAGCGGCCGCTCCAGGAGGAGGTGCTGAGG-3 (*Not*I site underlined) | 5-GGAGGAGTCGACTCCAAAGCTGTCCACCGTGA-3 (*Sal*I site underlined) | 581 |
| **Two different sets of morpholinos used for *trip4* and *ascc1* knockdown** | | | | |
| *trip4* | *MO* | 5-ATTGGTGCACACCTGAATGATGTGC-3 | | |
| *ascc1* | *MO* | 5-TGCACCTGTGACCACTGAGAGAAC-3 | | |
| *trip4* | *MO2* | 5-AGTGCGAGCTCACCAGACTGCCGCA-3 | | |
| *ascc1* | *MO2* | 5-ATACACTGACTTGTAAAGCACACTG-3 | | |
| *bactin* | *MO* | 5-CCTCTTACCTCAGTTACAATTTATA-3 | | |
| **Primers used for RT-PCR quantification of *trip4*, *ascc1*, and control (*bactin*) mRNA abundance after MO and MO2-knockdown** | | | | |
| *trip4* | *Ex4-5* | 5-CTCCCATTGACTTAATGAAGGCAC-3 | 5-GGTTCCCTCTCCCATCAG-3 | |
| *ascc1* | *Ex2-4* | 5-GCAGCAGTGGATCAGTGTC-3 | 5-CCCTGAGTCCTGTGAGC-3 | |
| *bactin* | *Ex1-2* | 5-CCTTCCTTCCTGGGTATGG-3 | 5-GGGGGAGCAATGATCTTGATC-3 | |
| **Primers used for cloning of full length *trip4* and *ascc1* constructs and for site directed mutagenesis** | | | | |
| *trip4* | *cloning* | 5-GGAATTCGCCGCCACC**ATG**AGCGATTCTTTGCTTCGCT GGAC-3 (start codon underlined) | 5-GCTCGAG**TCA**CGCTGGCTGCATTAAACACTT CTTG-3 (stop codon underlined) | 1784 |
| *trip4* | p.K265* | 5-GAATTTGACAAGAACAGTGTT**T**AGAGAACACAAGTCT TG-3 (mutant residue underlined) | 5-CAAGACTTGTGTTCTCT**A**AACACTGTTCTTGT CAAATTC -3 (mutant residue underlined) | |
| *ascc1* | *cloning* | 5-GAATCGATGCCGCCACC**ATG**GAGGTCTTACGGCCGCC-3 (start codon underlined) | 5-GTCTAGA**TCA**TGAGAATGTGATGTGTCCGGCTG-3 (stop codon underlined) | 1165 |
| *ascc1* | *fs* | 5-CGATGCTCATAACATAG**G**AGCAGACGGAC-3 (inserted nucleotides underlined) | 5-GTCCGTCTGCT**C**CTATGTTATGAGCATCG-3 (inserted nucleotides underlined) | |

## Antibodies for immunostaining, immunoprecipitation, and Western blot

***Table S9.*** **List of used antibodies**

| AB against | Species | Raised in species | Company | Order number |
|---|---|---|---|---|
| TRIP4 | Humans | Rabbit-pAB (IgG) | ATLAS | HPA016605 |
| ASCC1 | Humans | Goat-pAB (IgG) | Santa Cruz | sc-160156 |
| ASCC2 | Humans | Rabbit-pAB (IgG) | Sigma/Prestige | HPA001439 |
| CSRP1 | Humans | Rabbit-pAB (IgG) | Abcam | ab70010 |
| CALR | Humans | Rabbit-mAB (IgG), clone EPR3924 | Millipore | MABT145 |
| SP1 | Humans | Rabbit-pAB | Millipore | 07-645 |
| $MHC_{fast}$ | Humans | Rabbit-mAB (IgG1) | Novocastra/Leica | Clone: WB-MHCf |
| $MHC_{slow}$ | Humans | Rabbit-mAB | Novocastra/Leica | Clone: WB-MHCs |
| $MHC_{neo}$ | Humans | Rabbit-mAB (IgG1) | Novocastra/Leica | Clone: WB-MHCn |
| $MHC_{dev}$ | Humans | Rabbit-mAB (IgG1) | Novocastra/Leica | Clone: WB-MHCd |
| GAPDH | Humans | Mouse-mAB (IgG1) | Ambion/Applied Biosystems | AM4300, Clone: 6C5 |
| β-Tubulin | Humans | Rabbit-pAB (IgG) | Abcam | ab6046 |
| pan-Actin | Humans | Mouse-mAB (IgG1), clone C4 | Chemicon international | MAB1501R |
| znp-1 | Zebrafish | Mouse-mAB (IgG2a,κ) | DSHB | znp-1 |
| | | AlexaFluor594-α-Bungarotoxin | Life Technologies/Molecular Probes | B-13423 |
| | | Protein G Sepharose 4B | Life Technologies | 101241 |